slower than that for CZ silicon. This is explicable by the fact that the concentration of interstitial oxygen in as-grown MCZ silicons is smaller than that in as-grown CZ silicons. For isochronal annealing, the precipitate density in MCZ silicon increases at first with temperature then decreases above 923 K, while the tendency towards small density with CZ silicon occurs at a relatively lower temperature, since precipitates with larger size than the critical radius grow up more rapidly in CZ silicon than those in MCZ silicon under the same thermal conditions. Mai *et al.* (1990) have reported that thermal donor generation in MCZ silicon is much lower than in CZ silicon. All these factors confirm the above arguments, *i.e.* MCZ silicon is more thermally stable than CZ silicon. Furthermore, this confirms the observation that magnetic fields can effectively control the oxygen concentration. Since the oxygen concentration in MCZ silicon is smaller than that in CZ silicon, they have different thermal behaviours.

5. Concluding remarks

We have investigated the thermal behaviour of oxygen in silicon by analysing the *Pendellösung* fringes in X-ray section topographs. For isothermal annealing at 1023 K, the average size of precipitates increases with the annealing time while the precipitate density decreases. The precipitation approaches a saturation level after 250 h annealing for MCZ silicon. For isochronal annealing for 18 h, the size of precipitates increases rapidly with increasing temperature. This results from both the diffusivity of the interstitial oxygen and the critical radius of precipitates being larger at higher temperature. Comparison of the results for MCZ silicon with those for CZ silicon shows that MCZ silicon crystals are more thermally stable than CZ silicons. The thermal donor generation is also weaker in MCZ silicons than in CZ silicons. This suggests that magnetic fields can control the oxygen concentration effectively and can provide high-quality silicon crystals. Moreover, the MCZ and the CZ silicons have different thermal behaviours. The method described here provides a powerful technique for detecting microdefects of nanometre size and random distribution. This represents an important extension of X-ray topography to the field of crystal-defect characterization.

This work was supported by the National Natural Science Foundation of China.

References

CLAEYS, C. & VANHELLEMONT, J. (1993). *J. Cryst. Growth*, **126**, 41–49.
DEDERICHS, P. H. (1973). *J. Phys. F*, **3**, 471–475.
GÖSELE, U. & TAN, T. Y. (1982). *Appl. Phys.* A**28**, 79–82.
IIDA, S., SUGIYAMA, H., SUGITA, Y. & KAWATA, H. (1988). *Jpn. J. Appl. Phys.* **27**, 1081–1087.
KATO, N. (1980). *Acta Cryst.* A**36**, 763–769, 770–778.
MAI, Z. H., CUI, S.-F., WANG, C.-Y., WU, L.-S., LI, H.-P., CHEN, G.-X., ZHOU, S.-R. & YE, S.-C. (1990). *Mod. Phys. Lett.* B**4**, 625–634.
PATEL, J. R. (1973). *J. Appl. Phys.* **44**, 3903–3907.
SUGITA, Y., SUGIYAMA, H., IIDA, S. & KAWATA, H. (1987). *Jpn. J. Appl. Phys.* **26**, 1903–1906.

Acta Cryst. (1994). A**50**, 730–736

The Reduction of *N*-Beam Scattering from Noncentrosymmetric Crystals to Two-Beam Form

BY A. F. MOODIE AND H. J. WHITFIELD

Department of Applied Physics, Royal Melbourne Institute of Technology, Box 2476 *W, Melbourne, Victoria* 3001, *Australia*

(*Received* 8 *February* 1994; *accepted* 6 *April* 1994)

Abstract

It is shown that certain noncentrosymmetric seven-beam configurations can be reduced to two-beam form. This is exemplified for the space group of α-quartz, namely $P3_121$, with the incident beam along [001]. Explicit eigenvalues and eigenvectors are given for this case and it is shown that the two-beam form is independent of the imaginary parts of the structure amplitudes. The reduction is shown to result from five zero projectors rather than confluence, although confluence is present. An exhaustive list of the 15 reducible noncentrosymmetric space groups is obtained.

1. Introduction

When the probability of scattering more than once within the volume of a specimen is negligible, the relationship between the object and the scattered wavefield assumes the simple form of a Fourier transform. Inherent in the simplicity of this result lies the difficulty of recovering the phase of the scattered wavefield. For the weak interactions experienced by photons and neutrons, this single-scattering approximation can be extremely effective but for the strong interaction associated with electron scattering it has very limited validity. Under many circumstances, the approximation most likely to have some validity, that is the two-beam approximation, is of entirely different character. Whereas the kinematical approximation involves one term in the Born series, the two-beam dynamical approximation involves an infinite summation over scattering processes of restricted character. Again the solution is of explicit type and again it contains no phase information. Its range of application is however very great as standard texts on electron scattering testify. A brief outline has been given by Cowley & Moodie (1992).

The conditions under which the form of the two-beam solution can have some validity at first sight appear to be prohibitively restrictive. In effect, it is required that the only significant reflections should be those from the same set of Bragg planes. In practice, under accelerating voltages of approximately 80 kV or more, this condition is never satisfied to an accuracy of better than 2 or 3%: N-beam diffraction is, in fact, dominant. However, under a range of important practical conditions, the N-beam wavefield to good approximation reduces to two-beam form. This may happen in one of two ways: as a perturbation of strong beams by weak beams described by a pseudopotential (Bethe, 1928; Gjønnes, 1962) or by the amalgamation of symmetrically disposed strong beams (Niehrs, 1961; Blume, 1966; Fukuhara, 1966; Kogiso & Takahashi, 1977). Both reductions have general importance, the latter, for instance, in zone-axis critical-voltage effects, in the analysis of dislocation contrast and in the interpretation of certain zone-axis convergent-beam diffraction patterns.

Hitherto, it has been accepted that reduction is not possible in the absence of a centre of symmetry. The reasons for this assumption are not clear to us but may derive from one of the techniques used in such reductions. This particular method works successfully for the three-beam and by extension to both the five- and the seven-beam cases when a centre of symmetry is present. However, the three-beam symmetric case is not reducible in the absence of a centre of symmetry and the assumption appears to have been made that if the three-beam case is not reducible then no case of a greater number of beams will be.

In the present communication, it is shown that the greater flexibility offered by a seven-beam case is sufficient in 15 space groups to overcome the lack of a centre of inversion. Amongst the symmetry elements, the centre of inversion in many ways plays a special role. For instance, in the approximation for no back scattering, which concerns us in the present paper, the formal correspondence with the non-relativistic time-dependent equation of quantum mechanics is exact when the appropriate coordinate replaces the time coordinate.

2. Outline of the calculation

In general, Friedels's law is violated for noncentrosymmetric systems in which N-beam dynamical scattering is appreciable. Other symmetries may, however, override the lack of a centre of inversion, leading in extreme cases to complete reduction of the intensity to two-beam form. A necessary but insufficient condition for this is provided by the requirement that $\langle g|M^2|0\rangle/V_g$ should be real (Moodie & Fehlmann, 1993).

Reduction to two-beam form is carried out for the space group $P3_121$. Extension to 14 other space groups lacking a centre of symmetry and numerical results for reducible and irreducible space groups are described in § 6.

For the space group $P3_121$, M_o, the matrix describing scattering in the seven-beam approximation for radiation incident along the [001] direction, is given by

$$M_0 = \begin{bmatrix} 0 & V & V & V & V & V & V \\ V & \zeta & V & V_1^* & V_2 & V_1 & V \\ V & V & \zeta & V & V_1 & V_2 & V_1^* \\ V & V_1 & V & \zeta & V & V_1^* & V_2 \\ V & V_2 & V_1^* & V & \zeta & V & V_1 \\ V & V_1^* & V_2 & V_1 & V & \zeta & V \\ V & V & V_1 & V_2 & V_1^* & V & \zeta \end{bmatrix},$$

where V has been written for σV_{100} and ζ for $\pi\zeta$, $\sigma = (\pi/W\lambda)\{2/[1+(1-\beta_2)^{1/2}]\}$, $\beta = v/c$ and W is the accelerating voltage. The labelling of the structure amplitudes $V(hk0)$ is given in Fig. 1 and the ordering in Table 1.

For the eigenvectors $|^j\varphi_g\rangle$ corresponding to eigenvalues λ_j, the final wave function in reciprocal space is written as $\langle g|U\rangle$ so that the relation of Fujimoto (1959) can be written $U_g = \sum_j {}^j\varphi_o{}^{*j}\varphi_g \exp(i\lambda_j z)$ or $\langle g|U\rangle = \sum_j \langle {}^j\varphi|0\rangle\langle g|{}^j\varphi\rangle \exp(i\lambda_j z)$.

For the present system, then, with λ_l an eigenvalue, $\langle 1|M_0^2|0\rangle/V = \zeta + 2V + V_2 + (V_1 + V_1^*) = \lambda_N +$

Table 1. *Ordering scheme used in calculation*

g	*hkl*
0	000
1	010
2	100
3	1$\bar{1}$0
4	0$\bar{1}$0
5	$\bar{1}$00
6	$\bar{1}$10

λ_{N-1} so that it is possible that the system is reducible. In fact, the eigenvalues can be obtained explicitly, the reduction follows, and an application of Zassenhaus's theorem can be used to extend the treatment to the description of convergent-beam diffraction patterns.

3. Determination of the eigenvalues

The matrix M_0 can be decomposed into the sum of two commuting matrices, namely

$$M_1 = \begin{bmatrix} -S & V & V & V & V & V & V \\ V & 0 & 0 & 0 & 0 & 0 & 0 \\ V & 0 & 0 & 0 & 0 & 0 & 0 \\ V & 0 & 0 & 0 & 0 & 0 & 0 \\ V & 0 & 0 & 0 & 0 & 0 & 0 \\ V & 0 & 0 & 0 & 0 & 0 & 0 \\ V & 0 & 0 & 0 & 0 & 0 & 0 \end{bmatrix}$$

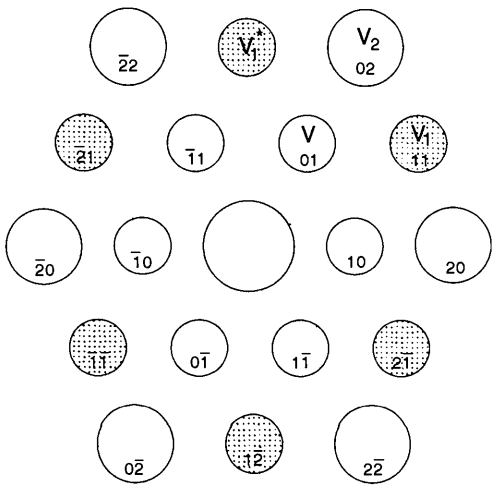

Fig. 1. Indexing scheme for the *ab* plane used in the calculation for space groups 150, 152, 154, 157, 159, 189 and 190. Dotted discs indicate complex structure amplitudes. For space groups 160 and 161, the inner beams are relabelled (1,1) (2,$\bar{1}$) (1,$\bar{2}$) ($\bar{1}$,$\bar{1}$) ($\bar{2}$,1) and ($\bar{1}$,2). For space groups 215, 217, 218 and 220, these beams are relabelled (01$\bar{1}$) (10$\bar{1}$) (1$\bar{1}$0) (0$\bar{1}$1) ($\bar{1}$01) and ($\bar{1}$10). For space groups 216 and 219, these beams are relabelled (02$\bar{2}$) (20$\bar{2}$) (2$\bar{2}$0) (0$\bar{2}$2) ($\bar{2}$02) and ($\bar{2}$20), with consistent relabelling of the outer beams.

and

$$M_2 = \begin{bmatrix} S & 0 & 0 & 0 & 0 & 0 & 0 \\ 0 & \zeta & V & V_1^* & V_2 & V_1 & V \\ 0 & V & \zeta & V & V_1 & V_2 & V_1^* \\ 0 & V_1 & V & \zeta & V & V_1^* & V_2 \\ 0 & V_2 & V_1^* & V & \zeta & V & V_1 \\ 0 & V_1^* & V_2 & V_1 & V & \zeta & V \\ 0 & V & V_1 & V_2 & V_1^* & V & \zeta \end{bmatrix},$$

$$\equiv \begin{bmatrix} S & 0 & 0 & 0 & 0 & 0 & 0 \\ 0 & & & & & & \\ 0 & & & & & & \\ 0 & & & M_3 & & & \\ 0 & & & & & & \\ 0 & & & & & & \\ 0 & & & & & & \end{bmatrix},$$

with $S=\zeta+2V+V_2+(V_1+V_1^*)$. The eigenvalues of M_1 are $(-S/2)\pm[(S/2)^2+6V^2]^{1/2}$, 0, 0, 0, 0, 0.

In the centrosymmetric case, M_3 is a circulant that can be diagonalized by the matrix F with entries given by $a_{ij}=6^{-1/2}\ \omega^{(i-1)(j-1)}$ (Appendix I), where the ω are the sixth roots of unity. In the present case, M_3 is not a circulant but the sum of each row and each column of M_3 is equal to S, so that M_3 belongs to the algebra $M_{1,2}$ (Davis, 1979). The centre of this algebra is a matrix, J, with every element equal to unity. This matrix, and hence M_3, is reduced to block form by the matrix F. The off-diagonal terms of the resultant block-form matrix depend only on the imaginary part of the structure amplitude V_1. The resulting block form is readily diagonalized, so that if one writes $V_1 \equiv a+ib$, the eigenvalues of M_2 are $\zeta+2V+V_2+2a$, $\zeta+2V+V_2+2a$, $\zeta-2V-V_2+2a$, $(\zeta-a)\pm[(V-V_2)^2+3b^2]^{1/2}$, $(\zeta-a)\pm[(V-V_2)^2+3b^2]^{1/2}$.

Since $[M_1,M_2]=0$, the eigenvalues of M_0 are the sum of the eigenvalues of M_1 and M_2, the order of addition being determined by the requirement that $\langle 1|M_0^2|0\rangle/V=\lambda_N+\lambda_{N-1}$.

In this way, the eigenvalues for M_0 are found to be

$$\lambda_1=\tfrac{1}{2}(\zeta+2V+V_2+2a)+[\tfrac{1}{4}(\zeta+2V+V_2+2a)^2+6V^2]^{1/2}$$
$$\equiv(S/2)+[(S/2)^2+6V^2]^{1/2}$$
$$\equiv 6^{1/2}V\alpha_+/\alpha_-$$
$$\lambda_2=\tfrac{1}{2}(\zeta+2V+V_2+2a)-[\tfrac{1}{4}(\zeta+2V+V_2+2a)^2+6V^2]^{1/2}$$
$$\equiv(S/2)-[(S/2)^2+6V^2]^{1/2}$$
$$\equiv -6^{1/2}V\alpha_-/\alpha_+$$
$$\lambda_3=(\zeta-a)+[(V-V_2)^2+3b^2]^{1/2},$$

$$\lambda_4=(\zeta-a)-[(V-V_2)^2+3b^2]^{1/2},$$
$$\lambda_5=\zeta-2V-V_2+2a,$$
$$\lambda_6=(\zeta-a)-[(V-V_2)^2+3b^2]^{1/2},$$
$$\lambda_7=(\zeta-a)+[(V-V_2)^2+3b^2]^{1/2}.$$

4. Determination of the eigenvectors

In order to facilitate comparison with the centrosymmetric case, we extend the notation of Fukuhara (1966) and define $\alpha\equiv(\zeta+2V+V_2+2a)/2V)$ and $\alpha_\pm\equiv\{(1/12)[1\pm\alpha/(\alpha^2+6)^{1/2}]\}^{1/2}$. The eigenvectors are then found to be (Appendix II)

$$\begin{bmatrix} 6^{1/2}\alpha_- & -6^{1/2}\alpha_+ & 0 & 0 & 0 & 0 & 0 \\ \alpha_+ & \alpha_- & \Gamma_- & \Gamma_- & 6^{-1/2} & \Gamma_+ & \Gamma_+ \\ \alpha_+ & \alpha_- & \Gamma_+\omega^5 & \Gamma_+\omega^4 & 6^{-1/2}\omega^3 & \Gamma_-\omega^2 & \Gamma_-\omega \\ \alpha_+ & \alpha_- & \Gamma_-\omega^4 & \Gamma_-\omega^2 & 6^{-1/2} & \Gamma_+\omega^4 & \Gamma_+\omega^2 \\ \alpha_+ & \alpha_- & \Gamma_+\omega^3 & \Gamma_+ & 6^{-1/2}\omega^3 & \Gamma_- & \Gamma_-\omega^3 \\ \alpha_+ & \alpha_- & \Gamma_-\omega^2 & \Gamma_-\omega^4 & 6^{-1/2} & \Gamma_+\omega^2 & \Gamma_+\omega^4 \\ \alpha_+ & \alpha_- & \Gamma_+\omega & \Gamma_+\omega^2 & 6^{-1/2}\omega^3 & \Gamma_-\omega^4 & \Gamma_-\omega^5 \end{bmatrix},$$

where $\Gamma_\pm\equiv 6^{-1/2}(2^{-1/2}\gamma_+\pm 2^{-1/2}\gamma_-)$, $\gamma_\pm\equiv[1\pm\gamma(\gamma^2+1)^{-1/2}]^{1/2}$ and $\gamma=(V-V_2)/(3^{1/2}b)$.

The two-beam nature of the solution derives directly from the form of the eigenvalues and eigenvectors since $\langle g|U\rangle=\sum_j\langle{}^j\varphi|0\rangle\langle g|{}^j\varphi\rangle\exp(i\lambda_j z)$ (Fujimoto, 1959). If ζ is replaced with $\pi\zeta$ and V with σV_{100}, then the explicit two-beam solution is given by

$$\langle 1|U\rangle = i\sigma V\exp[i(S/2)z]\times\frac{\sin[(S/2)^2+(6^{1/2}\sigma V)^2]^{1/2}z}{[(S/2)^2+(6^{1/2}\sigma V)^2]^{1/2}}$$

$$\langle 0|U\rangle=\exp[i(S/2)z]\left\{\cos[(S/2)^2+(6^{1/2}\sigma V)^2]^{1/2}z - i(S/2)\frac{\sin[(S/2)^2+(6^{1/2}\sigma V)^2]^{1/2}z}{[(S/2)^2+(6^{1/2}\sigma V)^2]^{1/2}}\right\},$$

where $S=2\pi\zeta+2\sigma V+\sigma V_2+2\sigma a$.

5. Discussion of the results

The condition $\langle 1|M^2|0\rangle/V_{100}=\lambda_N+\lambda_{N+1}$ derives from the requirement that $N-2$ of the projectors should be zero; explicit calculation (§ 4) showed that, indeed, ${}^j\varphi_o=0$ for $j=3, 4, 5, 6, 7$. The reduction is therefore not due to confluence, although confluence is present. A comparison can be made with the reduction of the three-beam centrosymmetric case, where straight-line loci in ζ make ${}^j\varphi_o$ zero. Confluence in this case arises only at the intersection of the loci, namely the Gjønnes point (Moodie, 1979).

The two-beam wave function is seen to be independent of b, the imaginary part of V_{110}; this might have been anticipated from the structure of M_0, which allows decomposition into two commuting matrices, one of which is independent of b and possesses only two nonzero eigenvalues.

It is shown in § 6 that, for specific orientations, reduction to two-beam form can in fact be obtained in 15 noncentrosymmetric space groups. In this category are the [111] projections of certain noncentrosymmetric cubic space groups. When b is put equal to zero, one of these reduces to the case considered by Blume (1966); his solution is then identical with that given here.

The approximately reducible case of a zone-axis convergent-beam diffraction pattern can be examined by applying Zassenhaus's theorem (as quoted by Magnus, 1954) to Sturkey's (1972) solution for fast electron scattering without upper-layer-line interaction. This procedure is described by Anstis, Lynch, Moodie & O'Keefe (1973) and leads to

$$\exp(iMz)=\exp(iM_0z)\exp[i\Delta(\zeta)z]\exp[-\tfrac{1}{2}(M_0,\Delta)(iz)^2]\ldots.$$

If the convergence of the incident beam is chosen so that the orders of diffraction partly overlap, then the intensities in the overlapped regions will depend on the coherence of the incident wave.

6. Application to other space groups

For 15 distinct non-centrosymmetric trigonal, hexagonal and cubic space groups, there exist two-dimensional projections along appropriate directions that have symmetry $p31m$; these are the [001] projections of trigonal space groups 150, 152, 154, 157, 159, 160 and 161 and hexagonal space groups 189 and 190 and the [111] projections of the cubic space groups 215, 216, 217, 218, 219 and 220. For these specific projections of the 15 space groups, seven-beam Niehrs reductions to an equivalent two-beam set are enumerated.

The explicit expressions for the two-beam case for specific projections of the other space groups can be obtained by a relabelling of the expressions derived in § 4 for space group 152. In this section, we demonstrate how this relabelling is achieved.

Group I: *trigonal space groups* 150, 152, 154, 157, 159, 160 *and* 161

Of the 25 trigonal space groups, eight in crystal classes $\bar{3}$ and $\bar{3}m$ are centrosymmetric. The 17 noncentrosymmetric space groups are divided conveniently into three groups according to whether the special projection along [001] has two-dimensional space-group symmetry $p31m$, $p3m1$ or $p3$. Calcula-

tion of the two-dimensional structure factors for each of the three groups shows that only for the group with $p31m$ symmetry does the set of six beams (0,1) (1,0) (1,$\bar{1}$) (0,$\bar{1}$) ($\bar{1}$,0) and ($\bar{1}$,1) together with the central beam undergo Niehrs reduction to an equivalent two-beam set for radiation incident along the z axis and neglected higher-layer-line effects.

(*a*) For the group of space groups 150, 152, 154, 157 and 159, the coordinates of a [001] projection of their equivalent general position are the same, namely x,y; $\bar{y},x-y$; $y-x,\bar{x}$; y,x; $\bar{x},y-x$; $x-y,\bar{y}$. For this set of coordinates with projection symmetry $p31m$, the six beams (0,$\bar{1}$) ($\bar{1}$,0) ($\bar{1}$,1) (0,1) (1,0) and (1,$\bar{1}$) form an equivalent two-beam set with the central beam.

(*b*) The space groups 160 and 161 also have projection symmetry $p31m$ along [001]. The atom coordinates of their equivalent 18-fold general positions projected along [001] are given by applying the rhombohedral lattice translations to the coordinates x,y; $\bar{y},x-y$; $y-x,\bar{x}$; $\bar{y},\bar{x}$; $x,x-y$; $y-x,y$. The rhombohedral lattice centring condition results in $A=B=0$ for beams with $-h+k\neq 3n$ for the [001] projection. For these space groups, the set of beams (1,1) (2,$\bar{1}$) (1,$\bar{2}$) ($\bar{1}$,$\bar{1}$) ($\bar{2}$,1) and ($\bar{1}$,2) form a seven-beam set with the central beam (Table 2) that undergoes an equivalent two-beam reduction of the same form as the five trigonal space groups above but with relabelling of V, V_1 and V_2.

Group II: *hexagonal space groups* 189 *and* 190

Of the 27 hexagonal space groups, six are centrosymmetric, namely those with point-group symmetry (PGS) either 6/*m* (two space groups) or 6/*mmm* (four space groups). The 21 noncentrosymmetric space groups comprise those with PGS either 6 (seven space groups), 622 (six space groups), 6*mm* (four space groups), $\bar{6}m2$ (two space groups) or $\bar{6}2m$ (two space groups). Of these 21 noncentrosymmetric space groups, those with PGS 6, 622 and 6*mm* have centred projections along [001]. The only hexagonal space groups that have noncentrosymmetric projections along [001] are 187 ($P\bar{6}m2$), 188 ($P\bar{6}c2$), 189 ($P\bar{6}2m$) and 190 ($P\bar{6}2c$). The hexagonal space groups 189 and 190 have the projection symmetry $p31m$ along [001]. The atom coordinates of the general positions for this projection are x,y; $\bar{y},x-y$; $y-x,\bar{x}$; y,x; $\bar{x},y-x$; $x-y,\bar{y}$; with each point doubly occupied. These coordinates are identical with those of the initial five trigonal space groups considered above and so the same two-beam reduction results.

Group III: *cubic space groups* 215, 216, 217, 218, 219 *and* 220

There are 19 noncentrosymmetric cubic space groups that have projections along [111] of two-dimensional space-group symmetry $p3$, $p3m1$ or $p31m$. Those with $p31m$ are the six space groups 215, 216, 217, 218, 219 and 220 (all of PGS $\bar{4}3m$). For space groups 215, 217, 218 and 220, the six beams (01$\bar{1}$) (10$\bar{1}$) (1$\bar{1}$0) (0$\bar{1}$1) ($\bar{1}$01) and ($\bar{1}$10) form with the central beam a seven-beam set that reduces to an equivalent two-beam set that has the same form as

Table 2. *Tabulation of values of* $A=\sum\cos 2\pi(hx+ky)$ *and* $B=\sum\sin 2\pi(hx+ky)$

[001] projection of space groups 150, 152, 154, 157 and 159

For 010 beam, $A=2\cos 2\pi x+2\cos 2\pi y+2\cos 2\pi(x-y)$, $B=0$
For 020 beam, $A=2\cos 4\pi x+2\cos 4\pi y+2\cos 4\pi(x-y)$, $B=0$
For 110 beam, $A=2\cos 2\pi(x+y)+2\cos 2\pi(x-2y)+2\cos 2\pi(y-2x)$
$B=2\sin 2\pi(x+y)+2\sin 2\pi(x-2y)+2\sin 2\pi(y-2x)$

[001] projection of space groups 160 and 161

For 110 beam, $A=6\cos 2\pi(x+y)+6\cos 2\pi(x-2y)+6\cos 2\pi(y-2x)$, $B=0$
For 220 beam, $A=6\cos 4\pi(x+y)+6\cos 4\pi(x-2y)+6\cos 4\pi(y-2x)$, $B=0$
For 300 beam, $A=6\cos 6\pi x+6\cos 6\pi y+6\cos 6\pi(x-y)$
$B=6\sin 6\pi x-6\sin 6\pi y+6\sin 6\pi(x-y)$

[001] projection of space groups 189 and 190

For 010 beam, $A=4\cos 2\pi x+4\cos 2\pi y+4\cos 2\pi(x-y)$, $B=0$
For 020 beam, $A=4\cos 4\pi x+4\cos 4\pi y+4\cos 4\pi(x-y)$, $B=0$
For 110 beam, $A=4\cos 2\pi(x+y)+4\cos 2\pi(x-2y)+4\cos 2\pi(y-2x)$
$B=4\sin 2\pi(x+y)+4\sin 2\pi(x-2y)+4\sin 2\pi(y-2x)$

[001] projection of space groups 149, 151, 153, 156 and 158

For 010 beam, $A=2\cos 2\pi x+2\cos 2\pi y+2\cos 2\pi(x-y)$
$B=-2\sin 2\pi x+2\sin 2\pi y+2\sin 2\pi(x-y)$
For 100 beam, $A=2\cos 2\pi x+2\cos 2\pi y+2\cos 2\pi(x-y)$
$B=2\sin 2\pi x-2\sin 2\pi y-2\sin 2\pi(x-y)$

[111] projection of space groups 215, 217, 218 and 220

For 01$\bar{1}$ beam, $A=8\cos 2\pi(y-z)+8\cos 2\pi(x-y)+8\cos 2\pi(z-x)$, $B=0$
For 02$\bar{2}$ beam, $A=8\cos 4\pi(y-z)+8\cos 4\pi(x-y)+8\cos 4\pi(z-x)$, $B=0$
For 11$\bar{2}$ beam, $A=2\cos 2\pi(x+y-2z)+2\cos 2\pi(x-y+2z)+2\cos 2\pi\times(y-x+2z)+2\cos 2\pi(-x-y-2z)+2\cos 2\pi(z+x-2y)+2\cos 2\pi(z-x+2y)+2\cos 2\pi(x-z+2y)+2\cos 2\pi(-x-z-2y)+2\cos 2\pi(y+z-2x)+2\cos 2\pi(y-z+2x)+2\cos 2\pi(z-y+2x)+2\cos 2\pi(-y-z-2x)$
$B=2\sin 2\pi(x+y-2z)+2\sin 2\pi(x-y+2z)+2\sin 2\pi\times(y-x+2z)+2\sin 2\pi(-x-y-2z)+2\sin 2\pi(z+x-2y)+2\sin 2\pi(z-x+2y)+2\sin 2\pi(x-z+2y)+2\sin 2\pi(-x-z-2y)+2\sin 2\pi(y+z-2x)+2\sin 2\pi(y-z+2x)+2\sin 2\pi(z-y+2x)+2\sin 2\pi(-y-z-2x)$

[111] projection of space groups 216 and 219

For 02$\bar{2}$ beam, $A=8\cos 4\pi(y-z)+8\cos 4\pi(x-y)+8\cos 4\pi(z-x)$, $B=0$
For 04$\bar{4}$ beam, $A=8\cos 8\pi(y-z)+8\cos 8\pi(x-y)+8\cos 8\pi(z-x)$, $B=0$
For 22$\bar{4}$ beam, $A=2\cos 4\pi(x+y-2z)+2\cos 4\pi(x-y+2z)+2\cos 4\pi\times(y-x+2z)+2\cos 4\pi(-x-y-2z)+2\cos 4\pi(z+x-2y)+2\cos 4\pi(z-x+2y)+2\cos 4\pi(x-z+2y)+2\cos 4\pi(-x-z-2y)+2\cos 4\pi(y+z-2x)+2\cos 4\pi(y-z+2x)+2\cos 4\pi(z-y+2x)+2\cos 4\pi(-y-z-2x)$
$B=2\sin 4\pi(x+y-2z)+2\sin 4\pi(x-y+2z)+2\sin 4\pi\times(y-x+2z)+2\sin 4\pi(-x-y-2z)+2\sin 4\pi(z+x-2y)+2\sin 4\pi(z-x+2y)+2\sin 4\pi(x-z+2y)+2\sin 4\pi(-x-z-2y)+2\sin 4\pi(y+z-2x)+2\sin 4\pi(y-z+2x)+2\sin 4\pi(z-y+2x)+2\sin 4\pi(-y-z-2x)$

found for the trigonal and hexagonal space groups already considered (Table 2) but with relabelling of V, V_1 and V_2.

For space groups 216 and 219, the face-centring condition $h+k$, $k+l=2n$ means the six beams closest to the central beam in the [111] projection are the six beams $(02\bar{2})$ $(20\bar{2})$ $(2\bar{2}0)$ $(0\bar{2}2)$ $(\bar{2}02)$ and $(\bar{2}20)$ and these beams give an equivalent two-beam reduction with the central beam (Table 2). The form is the same as the previous cases but with relabelling of V, V_1 and V_2.

We note at this point that the values of A and B given in Table 2 for crystals of space group 216 are based on an assumed general 96-fold site symmetry 1. There exist materials of space group 216 in which the only occupied sites are the 4(a) and 4(b) sites of point-group symmetry $\bar{4}3m$, for example the sphalerite form of ZnS. V_1 is real for the 422 beam of this substance. There is thus still a two-beam reduction but a coherent convergent-beam diffraction pattern will not show trigonality in the overlap of the inner 202 beams.

In many substances, only a portion of the atoms in the asymmetric unit of the crystal cell are in general positions. In α-quartz, the Si atoms are in special positions and the scattering from them does not contribute to the asymmetry of a [001] projection; hence, the coherent convergent-beam effects due to asymmetry in this compound are correspondingly delicate.

Noncentrosymmetric trigonal, hexagonal and cubic space groups that have projection symmetry $p3m1$ or $p3$ down appropriate directions do not lead to two-beam form in the seven-beam approximation. To illustrate this, consider the [001] projection of space groups 149, 151, 153, 156 and 158, which has symmetry $p3m1$. The atom coordinates of the equivalent general positions are x,y; $\bar{y},x-y$; $y-x,\bar{x}$; $\bar{y},\bar{x}$; $x,x-y$; $y-x,y$. As seen in Table 2, V_{100} is complex and so does not meet the necessary condition that $\langle g|M^2|0\rangle/V_g$ should be real for a two-beam reduction (Moodie & Fehlmann, 1993).

As an aside, we note that projections along [001] of noncentrosymmetric tetragonal space groups leads to five-beam Niehrs reductions to equivalent two-beam form. However, [001] projections of tetragonal space groups are all centred.

We compare simulations, using Bloch-wave formalism, of convergent-beam patterns for [001] projections of two noncentrosymmetric space groups, namely 152 (α-quartz, SiO_2) and 188 (benitoite, $BaTi[Si_3O_9]$). The former, satisfying the squared matrix condition, should and in fact does reduce (Fig. 2). This has also been observed experimentally (Moodie & Fehlmann, 1993). The latter does not satisfy the squared-matrix condition and so should not and in fact does not reduce (Fig. 2). Indeed, there is a strong breakdown of Friedel's law in the inner beams.

The computations were performed on a Sun computer using programs of Stadelmann (1987).

7. Concluding remarks

We have shown that the absence of a centre of symmetry does not preclude reduction of seven-beam interactions to two-beam form in specific space groups. The solution obtained can constitute the starting point for the analysis of various critical-voltage effects and of image contrast in the electron

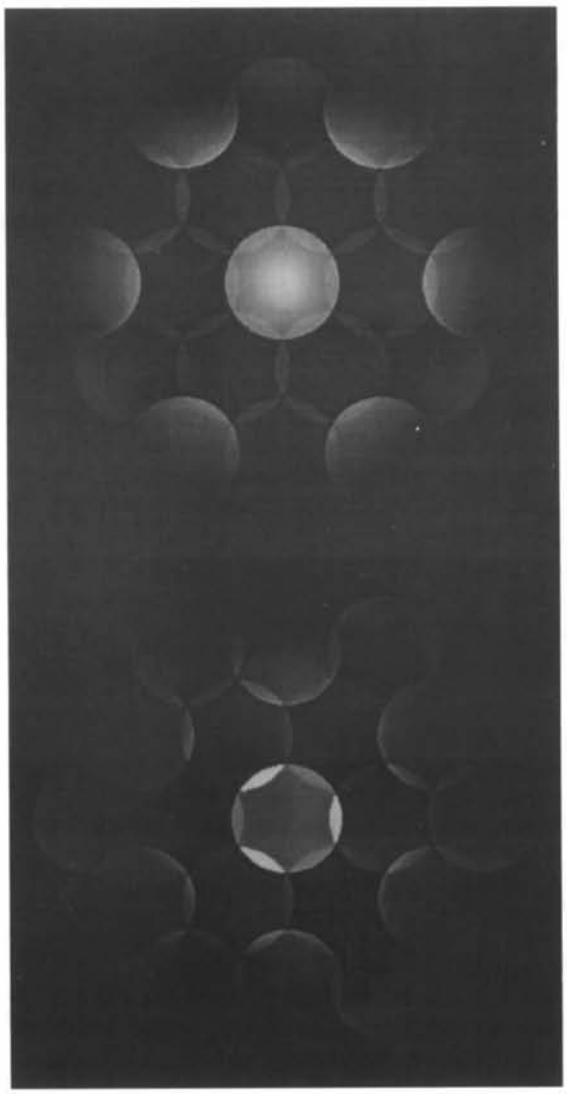

Fig. 2. Calculated convergent-beam electron diffraction patterns of 30 nm-thick crystals viewed down [001] of (top) α-quartz (SiO_2) and (bottom) benitoite, $BaTi[Si_3O_9]$. In each case, 55 beams were used in the Bloch-wave calculation.

microscope. As will be shown in subsequent publications, the results also influence the analysis of certain symmetry-induced effects in convergent-beam electron-diffraction patterns.

APPENDIX I
Eigenvalues

An nth-order circulant is diagonalized by the Fourier matrices, F, which are unitary and are the nth matrix roots of unity, *i.e.* $F^n = E$, or $a_{ij} = n^{-1/2}\,\omega^{(i-1)(j-1)}$. In the present case, M_3 is not a circulant but rather a member of the 'Magic' algebra $M_{1,2}$. This algebra is the centralizer of the matrix J that has every element unity. The eigenvalues of this matrix are n, 0, ..., 0, so that F reduces M_3 to a block-diagonal form (Davis, 1979). Hence,

$$F^{-1}M_3F = \begin{bmatrix} D_{11} & 0 & 0 & 0 & 0 & 0 \\ 0 & D_{22} & 0 & 0 & D_{25} & 0 \\ 0 & 0 & D_{33} & 0 & 0 & D_{36} \\ 0 & 0 & 0 & D_{44} & 0 & 0 \\ 0 & D_{52} & 0 & 0 & D_{55} & 0 \\ 0 & 0 & D_{63} & 0 & 0 & D_{66} \end{bmatrix} \equiv B,$$

where $D_{11} = S = \zeta + 2V + V_2 + 2a$, $D_{22} = D_{66} = \zeta + V - V_2 - a$, $D_{33} = D_{55} = \zeta - V + V_2 - a$, $D_{44} = \zeta - 2V - V_2 + 2a$, $D_{36} = D_{63} = -3^{1/2}\,b$ and $D_{25} = D_{52} = 3^{1/2}\,b$.

The characteristic equation for B can then be solved, giving the eigenvalues $\zeta + 2V + V_2 + 2a$, $\zeta - 2V - V_2 + 2a$, $(\zeta - a) \pm [(V - V_2)^2 + 3b^2]^{1/2}$, $(\zeta - a) \pm [(V - V_2)^2 + 3b^2]^{1/2}$. The eigenvalues for M_0 can then be written down, the order of addition being conveniently determined by the requirement $\langle 1|M_0^2|0\rangle/V = \lambda_N + \lambda_{N-1}$.

APPENDIX II
Eigenvectors

The eigenvectors of M_1 are conveniently expressed in terms of $\alpha_\pm \equiv \{(1/12)[1 \pm \alpha/(\alpha^2+6)^{1/2}]\}^{1/2}$, where $\alpha \equiv (\zeta + 2V + V_2 + 2a)/(2V) \equiv S/(2V)$. Similarly, the first eigenvalue $\lambda_1 = (S/2) + [(S/2)^2 + 6V^2]^{1/2} \equiv 6^{1/2}V\alpha_+/\alpha_-$. The eigenvectors of M_3 can be calculated by noting that the block-diagonal matrix B is diagonalized by

$$Q = \begin{bmatrix} 1 & 0 & 0 & 0 & 0 & 0 \\ 0 & g_+ & 0 & 0 & g_- & 0 \\ 0 & 0 & g_+ & 0 & 0 & g_- \\ 0 & 0 & 0 & 1 & 0 & 0 \\ 0 & -g_- & 0 & 0 & g_+ & 0 \\ 0 & 0 & -g_- & 0 & 0 & g_+ \end{bmatrix},$$

with $g_\pm = \gamma_\pm/2^{1/2}$, $\gamma_\pm \equiv [1 \pm \gamma(\gamma^2+1)^{-1/2}]^{1/2}$ and $\gamma = (V - V_2)/(3^{1/2}b)$, so that

$$g_\pm = 2^{-1/2}(1 \pm \{(V - V_2)/[(V - V_2)^2 + 3b^2]^{1/2}\})^{1/2}.$$

Thus, for the centrosymmetric case with $b = 0$, $g_+ = 1$ and $g_- = 0$. Since $Q^{-1}BQ = D$ (say), then $Q^{-1}F^{-1}M_3FQ = (FQ)^{-1}M_3(FQ) = D$ and

$$FQ = \begin{bmatrix} 1 & \Gamma_- & \Gamma_- & 6^{-1/2} & \Gamma_+ & \Gamma_+ \\ 1 & \Gamma_+\omega^5 & \Gamma_+\omega^4 & 6^{-1/2}\omega^3 & \Gamma_-\omega^2 & \Gamma_-\omega \\ 1 & \Gamma_-\omega^4 & \Gamma_-\omega^2 & 6^{-1/2} & \Gamma_+\omega^4 & \Gamma_+\omega^2 \\ 1 & \Gamma_+\omega^3 & \Gamma_+ & 6^{-1/2}\omega^3 & \Gamma_- & \Gamma_-\omega^3 \\ 1 & \Gamma_-\omega^2 & \Gamma_-\omega^4 & 6^{-1/2} & \Gamma_+\omega^2 & \Gamma_+\omega^4 \\ 1 & \Gamma_+\omega & \Gamma_+\omega^2 & 6^{-1/2}\omega^3 & \Gamma_-\omega^4 & \Gamma_-\omega^5 \end{bmatrix},$$

with $\Gamma_\pm \equiv 6^{-1/2}(2^{-1/2}\gamma_+ \pm 2^{-1/2}\gamma_-)$.

Since M_1 and M_2 commute, the nonzero eigenvalues of M_1 are also eigenvalues for M_0 and so the complete set is as tabulated in the text.

References

ANSTIS, G. R., LYNCH, D. F., MOODIE, A. F. & O'KEEFE, M. A. (1973). *Acta Cryst.* A**29**, 138–147.

BETHE, H. A. (1928). *Ann. Phys. (Leipzig)*, **87**, 55–129.

BLUME, J. (1966). *Z. Phys.* **191**, 248–272.

COWLEY, J. M. & MOODIE, A. F. (1992). *P. P. Ewald and his Dynamical Theory of Diffraction*, edited by D. W. J. CRUICKSHANK, H. W. JURETSCHKE & N. KATO, ch. 10. IUCr/Oxford Univ. Press.

DAVIS, P. J. (1979). *Circulant Matrices*, p. 214. New York: Wiley.

FUJIMOTO, F. (1959). *J. Phys. Soc. Jpn*, **14**, 1558–1568.

FUKUHARA, A. (1966). *J. Phys. Soc. Jpn*, **21**, 2645–2662.

GJØNNES, J. (1962). *Acta Cryst.* **15**, 703–707.

KOGISO, M. & TAKAHASHI, H. (1977). *J. Phys. Soc. Jpn*, **42**, 223–229.

MAGNUS, W. (1954). *Commun. Pure Appl. Math.* **7**, 649–673.

MOODIE, A. F. (1979). *Chem. Scr.* **14**, 21–22.

MOODIE, A. F. & FEHLMANN, M. (1993). *Acta Cryst.* A**49**, 376–378.

NIEHRS, H. (1961). International Conference on Magnetism and Crystallography, Kyoto, Japan. Paper No. 232.

STADELMANN, P. A. (1987). *Ultramicroscopy*, **21**, 131–146.

STURKEY, L. (1972). *Proc. Phys. Soc.* **80**, 321–354.